

## Effects of Additives on Solid State Reaction. III. Effects of Halide Additives on the Formation of $\text{MgFe}_2\text{O}_4$

Shiro SHIMADA, Ryusaburo FURUICHI, and Tadao ISHII

Department of Applied Chemistry, Faculty of Engineering, Hokkaido University, Sapporo 060

(Received July 3, 1975)

The promoting effects of halide additives on the formation of  $\text{MgFe}_2\text{O}_4$  have been studied on the basis of both kinetic and thermoanalytical data. A mixture of  $\text{MgO}$  and  $\alpha\text{-Fe}_2\text{O}_3$  powder containing 10 mol % additive ( $\text{LiF}$ ,  $\text{NaF}$ ,  $\text{MgF}_2$ ,  $\text{BaF}_2$ ,  $\text{NaCl}$ , or  $\text{KCl}$ ) and that without additive were isothermally heated in a vacuum ( $P_{\text{O}_2}=10^0\text{--}10^1$  mmHg) in the temperature range 666—1018 °C. High temperature X-ray analysis on  $\text{MgO-Fe}_2\text{O}_3$  and  $\text{MgO-Fe}_2\text{O}_3$ -additive systems was carried out at a heating rate of 3 °C/min *in vacuo*, ( $P_{\text{O}_2}=10^{-1}$  mmHg). In the case of fluoride, it seems that the reactions between the fluoride and the reactants,  $\alpha\text{-Fe}_2\text{O}_3$  or  $\text{MgO}$ , promote  $\text{MgFe}_2\text{O}_4$  formation in the initial stage and that compounds produced by the initial reaction accelerate diffusion in the later stage. The same promoting mechanism seems to be applicable to the case of chloride additives. The interaction between solids of  $\text{NaCl}$  and  $\alpha\text{-Fe}_2\text{O}_3$  occurring just before the melting of  $\text{NaCl}$  seems to initiate  $\text{MgFe}_2\text{O}_4$  formation.

Solid state reactions are affected by various factors such as impurity or additive,<sup>1,2)</sup> preparation history of the reacting material<sup>3)</sup> and atmosphere.<sup>4-6)</sup> The mechanism for the promoting effects of fluoride and chloride additives on  $\text{MgAl}_2\text{O}_4$  formation has been systematically discussed from kinetic and thermoanalytical viewpoints.<sup>7-9)</sup> In the case of fluoride additives,<sup>8,9)</sup> the formation of  $\text{MgAl}_2\text{O}_4$  was initiated by the reaction between fluoride and reactants of  $\alpha\text{-Al}_2\text{O}_3$  and  $\text{MgO}$ , the cations of fluoride playing an important role in accelerating the reaction in the later stage. In the case of chloride,<sup>7,8)</sup> the  $\text{MgAl}_2\text{O}_4$  formation was accelerated *via* the dissolution process of  $\text{MgO}$  particle in molten chloride.

We have investigated the promoting effects of the halides of alkali and alkaline earth on  $\text{MgFe}_2\text{O}_4$  formation on the basis of both kinetic and thermoanalytical results.

### Experimental

**Sample.**  $\alpha\text{-Fe}_2\text{O}_3$  samples were prepared by calcining commercial ferric oxide (Kanto Chemical Co., 99% pure) at 1100 °C in the air. The particle size of  $\alpha\text{-Fe}_2\text{O}_3$  was microscopically determined to be in the range 0.5—2  $\mu$  with an average size of 1  $\mu$ .  $\text{MgO}$  particles (av. 0.1  $\mu$ ) were prepared by a similar way to that described in the previous paper.<sup>8)</sup> Powders of  $\text{MgO}$ ,  $\alpha\text{-Fe}_2\text{O}_3$  and additive were thoroughly mixed in the molar ratio 1:1:0.1. The additives used were  $\text{LiF}$ ,  $\text{NaF}$ ,  $\text{MgF}_2$ ,  $\text{BaF}_2$ ,  $\text{NaCl}$ , or  $\text{KCl}$  (Kanto, Wako or Morita Companies), which were stored in a desiccator with silica gel before experiments. The mixtures were pressed into pellets at 150 kg/cm<sup>2</sup>.

**DTA and High Temperature X-Ray Diffraction Experiments.** DTA experiments on  $\text{MgO-Fe}_2\text{O}_3$  and  $\text{MgO-Fe}_2\text{O}_3$ -additive systems were carried out in a vacuum ( $P_{\text{O}_2}=10^{-1}$  mmHg) at a heating rate of 10 °C/min. The temperature was measured with a Pt-Pt13Rh thermocouple.  $\alpha\text{-Al}_2\text{O}_3$  was used as a standard material. The high temperature X-ray diffraction experiments were carried out *in vacuo* ( $P_{\text{O}_2}=10^{-1}$  mmHg) at a heating rate of 3 °C/min.

**Isothermal Kinetic Experiments.** The pellet was kept on a Pt boat placed in a fused-silica tube connected to a vacuum system ( $P_{\text{O}_2}=10^0\text{--}10^1$  mmHg) and then heated isothermally in the Pt-furnace at 666—1018 °C. The temperature was measured with a Pt-Pt13Rh thermocouple. After heating,

the pellet was quenched at room temperature by withdrawal of the tube from the hot zone of the furnace. Fractional conversion of  $\text{MgFe}_2\text{O}_4$  was determined by measuring the amount of  $\text{MgO}$  or  $\alpha\text{-Fe}_2\text{O}_3$  remaining after the reaction. The  $\text{MgO}$  unreacted was extracted by dissolving the pellet in 10%  $\text{NH}_4\text{Cl}$  solution. The  $\text{Mg}^{2+}$  ion concentration of the solution was then determined by titration with a standard solution of EDTA. This procedure was applied to the products obtained in the experiments of both  $\text{MgO-Fe}_2\text{O}_3$  and  $\text{MgO-Fe}_2\text{O}_3$ -additive ( $\text{LiF}$  or  $\text{NaF}$ ) systems. The amount of  $\alpha\text{-Fe}_2\text{O}_3$  unreacted was determined by quantitative X-ray analysis by use of  $\text{NaCl}$  as an external standard. The method was applied to the products in  $\text{MgO-Fe}_2\text{O}_3$ -additive ( $\text{MgF}_2$  or  $\text{BaF}_2$ ) system.

**Analysis of  $\text{Fe}^{2+}$ .** The amount of  $\text{Fe}^{2+}$  ion in the samples, obtained after isothermal experiments or the high temperature X-ray diffraction experiments, was colorimetrically determined.<sup>10)</sup> The solution for colorimetry was prepared by dissolving the sample in concd  $\text{H}_2\text{SO}_4$ , 2M  $\text{NH}_4\text{F}$  and 1% *o*-phenanthroline were used as masking agent for  $\text{Fe}^{3+}$  and color-producing agent for  $\text{Fe}^{2+}$ .

### Results

Figures 1 and 2 show the rates of  $\text{MgFe}_2\text{O}_4$  formation in  $\text{MgO-Fe}_2\text{O}_3$  and  $\text{MgO-Fe}_2\text{O}_3$ -alkali fluoride systems, and  $\text{MgO-Fe}_2\text{O}_3$ -alkaline earth fluoride system, respectively. The rate of reaction between solid reactant particles is generally governed by either chemical reaction at phase-boundary or diffusion process.<sup>11)</sup> The rate equations for the diffusion-controlled reaction have been given by Jander,<sup>12)</sup> Serin-Ellickson,<sup>13)</sup> Ginstling-Brounshtein,<sup>14)</sup> and Carter.<sup>15)</sup> It was found that the reaction rate of  $\text{MgO-Fe}_2\text{O}_3$  system is best represented by Jander's equation:

$$[1 - (1 - \alpha)^{1/3}]^2 = kt \quad (1)$$

where  $\alpha$ =fractional conversion,  $k$ =rate constant,  $t$ =reaction time. A part of the data plotted according to Eq. (1) is shown in Fig. 3. We see that the data of all systems fit Jander's equation up to about  $\alpha=70\%$ . The straight lines obtained for  $\text{NaF}$ ,  $\text{MgF}_2$  and  $\text{BaF}_2$  additives intersect at  $t=0$  the ordinate with values corresponding to  $\alpha=20\text{--}30\%$ . On the other hand, the lines for non-additive and  $\text{LiF}$  additive fall on the origin. The activation energies are given in Table 1,

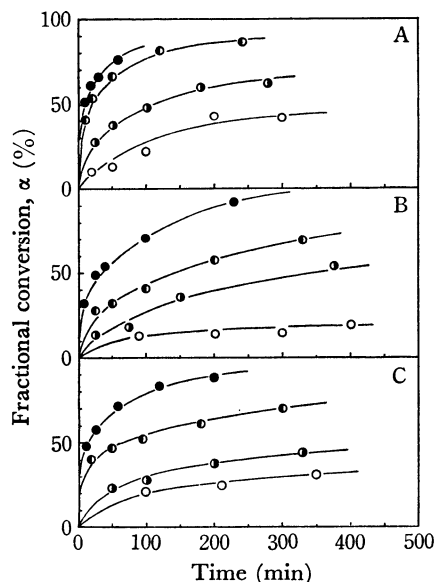


Fig. 1. Formation rate of  $\text{MgFe}_2\text{O}_4$  for  $\text{MgO-Fe}_2\text{O}_3$  and  $\text{MgO-Fe}_2\text{O}_3$ -alkali fluoride systems.

A:  $\text{MgO-Fe}_2\text{O}_3$  system  
 ○: 853 °C, ●: 915 °C, ●: 972 °C, ●: 1018 °C  
 B:  $\text{MgO-Fe}_2\text{O}_3$ -LiF system  
 ○: 666 °C, ●: 715 °C, ●: 760 °C, ●: 814 °C  
 C:  $\text{MgO-Fe}_2\text{O}_3$ -NaF system  
 ○: 754 °C, ●: 798 °C, ●: 850 °C, ●: 901 °C

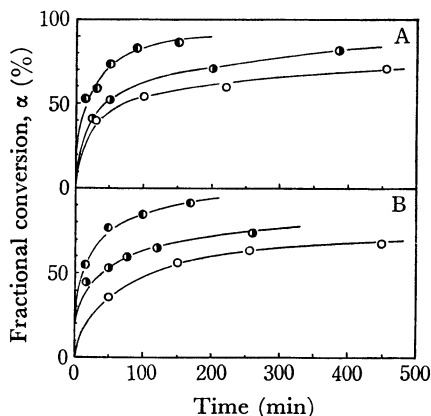


Fig. 2. Formation rate of  $\text{MgFe}_2\text{O}_4$  for  $\text{MgO-Fe}_2\text{O}_3$ -alkaline earth fluoride system.

A:  $\text{MgO-Fe}_2\text{O}_3$ - $\text{MgF}_2$  system  
 ○: 847 °C, ●: 895 °C, ●: 940 °C  
 B:  $\text{MgO-Fe}_2\text{O}_3$ - $\text{BaF}_2$  system  
 ○: 847 °C, ●: 895 °C, ●: 940 °C

for which the rate constants  $k$  were calculated from the results shown in Figs. 1 and 2 by means of Eq. (1). The samples obtained by the isothermal experiments of all systems showed no trace of  $\text{Fe}^{2+}$ .

Figure 4 shows DTA curves of  $\text{MgO-Fe}_2\text{O}_3$ -LiF (curve A) and  $\text{MgO-Fe}_2\text{O}_3$ -NaF (curve B) systems. Curve A has two endothermic peaks at 670 °C and 730 °C. The peak at 730 °C is considered to be due to the formation of the liquid phase, since an exothermic peak was obtained at *ca.* 730 °C by cooling the sample (curve A) from 930 °C as indicated by arrows. The liquid phase seems to result from melting of LiF.

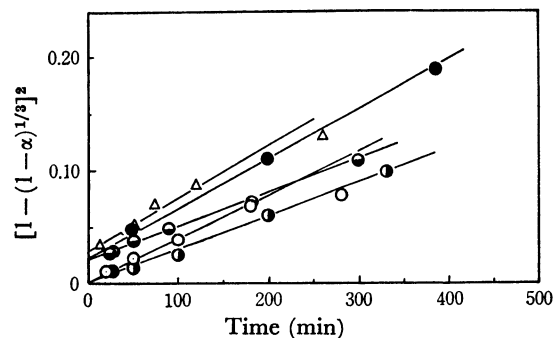


Fig. 3. Plots of  $[1 - (1 - \alpha)^{1/3}]^2$  vs.  $t$  according to the Jander's equation.

○: non-additive (915 °C), ●: LiF (760 °C), ●: NaF (850 °C) ●:  $\text{MgF}_2$  (895 °C), △:  $\text{BaF}_2$  (895 °C)

TABLE 1. VALUES OF ACTIVATION ENERGY

Additive	$E^*$ (kcal/mol)
Non-additive	$70 \pm 4$
LiF	$57 \pm 4$
NaF	$59 \pm 4$
$\text{MgF}_2$	$65 \pm 10$
$\text{BaF}_2$	$60 \pm 5$

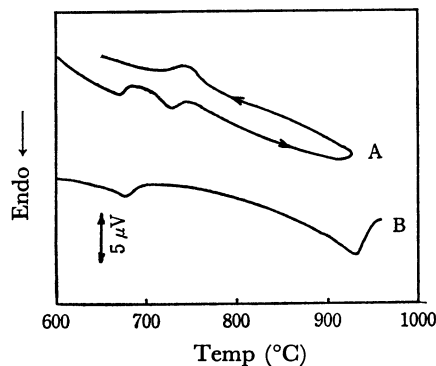


Fig. 4. DTA curves of reaction in  $\text{MgO-Fe}_2\text{O}_3$ -LiF (curve A) and  $\text{MgO-Fe}_2\text{O}_3$ -NaF (curve B) systems. Heating rate: 10 °C/min, sample weight: 400 mg, 1:1:0.1 mixture of  $\text{MgO}$ ,  $\text{Fe}_2\text{O}_3$ , and LiF or NaF in molar ratio.

Similarly, curve B has two endothermic peaks at 670 °C and 930 °C. The peak at 930 °C probably corresponds to melting of NaF. DTA curves of the systems with non-additive,  $\text{MgF}_2$  and  $\text{BaF}_2$  additives showed no thermal change in the range 20–1000 °C except for the endothermic peak near 670 °C, which showed a reversible one. This peak corresponds to the Curie point of  $\alpha\text{-Fe}_2\text{O}_3$ .<sup>16,17)</sup>

Figures 5A–D and 6A–D show the results of high temperature X-ray diffraction analysis for the systems  $\text{MgO-Fe}_2\text{O}_3$ ,  $\text{MgO-Fe}_2\text{O}_3$ -NaCl,  $\text{MgO-Fe}_2\text{O}_3$ -KCl,  $\text{Fe}_2\text{O}_3$ -NaCl,  $\text{MgO-Fe}_2\text{O}_3$ -LiF,  $\text{MgO-Fe}_2\text{O}_3$ -NaF,  $\text{MgO-Fe}_2\text{O}_3$ - $\text{MgF}_2$ , and  $\text{MgO-Fe}_2\text{O}_3$ - $\text{BaF}_2$ . We see that the amounts of  $\alpha\text{-Fe}_2\text{O}_3$  and  $\text{MgO}$  decrease at *ca.* 700 °C and then  $\text{MgFe}_2\text{O}_4$  begins to appear at 820 °C (Fig. 5-A). Addition of NaCl (Fig. 5-B) lowers the initiation temperature of  $\text{MgFe}_2\text{O}_4$  formation by more than 60 °C, as compared with that of the  $\text{MgO-Fe}_2\text{O}_3$  system. This initiation temperature, 760 °C, is lower

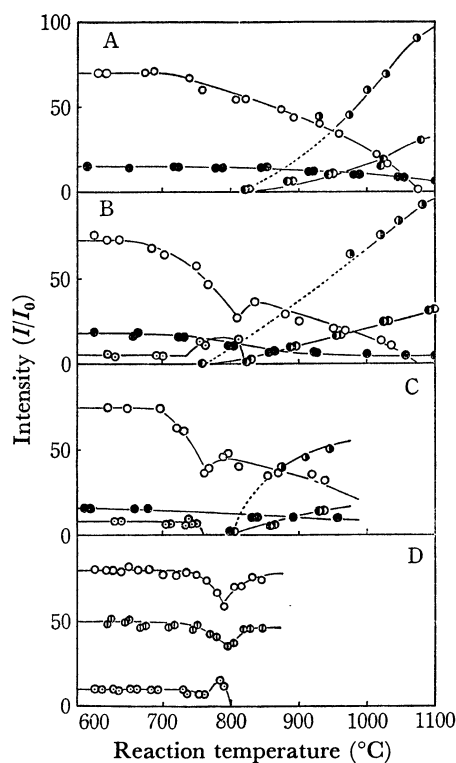


Fig. 5. High temperature X-ray diffraction patterns of the reaction in the systems for  $\text{MgO-Fe}_2\text{O}_3$  (A),  $\text{MgO-Fe}_2\text{O}_3\text{-NaCl}$  (B),  $\text{MgO-Fe}_2\text{O}_3\text{-KCl}$  (C), and  $\text{Fe}_2\text{O}_3\text{-NaCl}$  (D).

Molar mixing ratio: 1:1:0.1 in  $\text{MgO:Fe}_2\text{O}_3$ :chloride

and 1:0.2 in  $\text{Fe}_2\text{O}_3\text{:NaCl}$ , heating rate:  $3^\circ\text{C/min}$ .

○:  $\alpha\text{-Fe}_2\text{O}_3$  (104), ●:  $\text{MgO}$  (200), ◐ and ◑:  $\text{MgFe}_2\text{O}_4$  (311) and (200), respectively, B-◒:  $\text{NaCl}$  (200), C-◓:  $\text{KCl}$  (200), D-◐, -◑ and -◒:  $\alpha\text{-Fe}_2\text{O}_3$  (104),  $\alpha\text{-Fe}_2\text{O}_3$  (110) and  $\text{NaCl}$  (200), respectively.

than the melting point of  $\text{NaCl}$  (mp  $808^\circ\text{C}$ ). In the case of  $\text{KCl}$  (Fig. 5-C),  $\text{MgFe}_2\text{O}_4$  begins to form at *ca.*  $800^\circ\text{C}$  after melting of  $\text{KCl}$  (mp  $776^\circ\text{C}$ ). The discontinuous changes in the X-ray intensities of  $\alpha\text{-Fe}_2\text{O}_3$  and  $\text{NaCl}$  for  $\text{MgO-Fe}_2\text{O}_3\text{-NaCl}$  system (Fig. 5-B), and of  $\alpha\text{-Fe}_2\text{O}_3$  for  $\text{MgO-Fe}_2\text{O}_3\text{-KCl}$  system (Fig. 5-C) are observed just before the melting of chloride additives. Such phenomena are also observed in the binary system of  $\text{NaCl-Fe}_2\text{O}_3$  (Fig. 5-D). Addition of  $\text{LiF}$  (Fig. 6-A) lowers the initiation temperature of  $\text{MgFe}_2\text{O}_4$  formation to  $700^\circ\text{C}$ . This temperature is close to that of the liquid phase formation ( $730^\circ\text{C}$ ) in  $\text{MgO-Fe}_2\text{O}_3\text{-LiF}$  system (Fig. 4). In the case of  $\text{NaF}$  (Fig. 6-B), the initiation temperature is also lowered, the intensity of  $\text{MgFe}_2\text{O}_4$  increasing abruptly at  $1020^\circ\text{C}$ .

TABLE 2. THE INITIATION TEMPERATURE OF  $\text{MgFe}_2\text{O}_4$  FORMATION

Additive	Init. temp ( $^\circ\text{C}$ )
Non-additive	820
$\text{LiF}$	700
$\text{NaF}$	725
$\text{MgF}_2$	800
$\text{BaF}_2$	900
$\text{NaCl}$	760
$\text{KCl}$	800

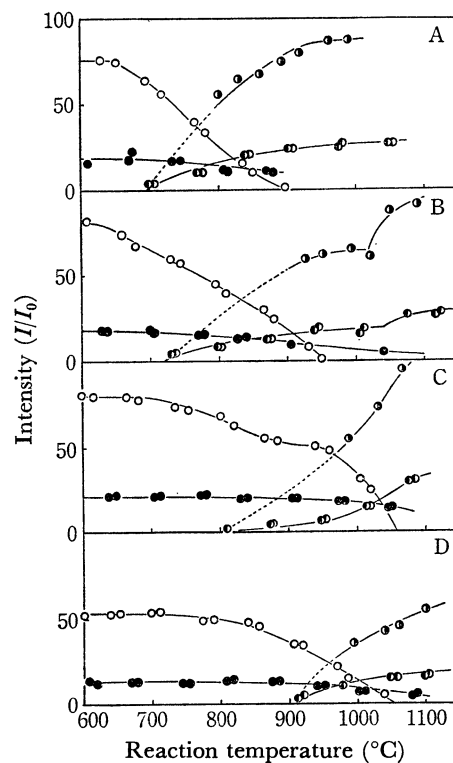


Fig. 6. High temperature X-ray diffraction patterns of the reaction in systems for  $\text{MgO-Fe}_2\text{O}_3\text{-LiF}$  (A),  $\text{MgO-Fe}_2\text{O}_3\text{-NaF}$  (B),  $\text{MgO-Fe}_2\text{O}_3\text{-MgF}_2$  (C) and  $\text{MgO-Fe}_2\text{O}_3\text{-BaF}_2$  (D).

Molar mixing ratio: 1:1:0.1, heating rate:  $3^\circ\text{C/min}$

○:  $\alpha\text{-Fe}_2\text{O}_3$  (104), ●:  $\text{MgO}$  (200), ◐ and ◑:  $\text{MgFe}_2\text{O}_4$  (311) and (200), respectively

In the case of  $\text{MgF}_2$  (Fig. 6-C),  $\text{MgFe}_2\text{O}_4$  begins to form at  $800^\circ\text{C}$ . On the other hand, the initiation temperature of the system with  $\text{BaF}_2$  (Fig. 6-D) is somewhat higher in comparison with that of other systems. The initiation temperatures of the  $\text{MgFe}_2\text{O}_4$  formation in all the systems are summarized in Table 2. It is seen that  $\alpha\text{-Fe}_2\text{O}_3$  in  $\text{MgO-Fe}_2\text{O}_3$  system disappears at temperatures higher than  $1075^\circ\text{C}$ , but  $\text{MgO}$  still exists at these temperatures (Fig. 5-A). Similar phenomena are also observed at  $1075^\circ\text{C}$ ,  $950^\circ\text{C}$ ,  $1060^\circ\text{C}$ , or  $1050^\circ\text{C}$  in  $\text{MgO-Fe}_2\text{O}_3\text{-NaCl}$ ,  $\text{-NaF}$ ,  $\text{-MgF}_2$ , or  $\text{-BaF}_2$ , respectively. The samples obtained after the high temperature X-ray diffraction experiments (Figs. 5-A, -B and 6-A, -B, -C, -D) showed traces of  $\text{Fe}^{2+}$ .

## Discussion

It was found<sup>9)</sup> that the lower the melting point of the fluoride additives, the lower the initial temperature of  $\text{MgAl}_2\text{O}_4$  formation, and that  $\text{AlF}_3$  formed by the reaction between fluorides and  $\alpha\text{-Al}_2\text{O}_3$  initiates the formation of  $\text{MgAl}_2\text{O}_4$ . For the  $\text{MgO-Fe}_2\text{O}_3\text{-fluoride}$  systems, a linear correlation of the melting point of the fluoride with the initiation temperature of  $\text{MgFe}_2\text{O}_4$  formation (Table 1) was also observed (Fig. 7). Deviation of the point for  $\text{BaF}_2$  from a straight line may be due to the poor crystallinity of  $\text{MgFe}_2\text{O}_4$  formed, since although the initial temperature of  $\text{MgFe}_2\text{O}_4$  formation is at *ca.*  $900^\circ\text{C}$  (Fig. 6-D), the fractional conversion

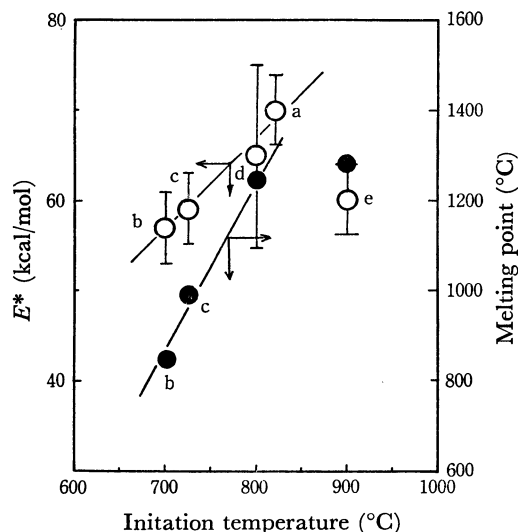


Fig. 7. Plots of the melting points of halide and the  $E^*$  values vs. the initiation temperature of  $\text{MgFe}_2\text{O}_4$  formation.

a: non-additive, b: LiF, c: NaF, d:  $\text{MgF}_2$ , e:  $\text{BaF}_2$

determined from the amount of unreacted  $\alpha\text{-Fe}_2\text{O}_3$  after the isothermal experiments goes up to  $\alpha=36\%$  at  $847^\circ\text{C}$  for 50 min in  $\text{MgO-Fe}_2\text{O}_3\text{-BaF}_2$  system. The correlation in Fig. 7 suggests that the fluoride of lower melting point easily reacts with reactants  $\alpha\text{-Fe}_2\text{O}_3$  or  $\text{MgO}$  and that the reaction promotes the  $\text{MgFe}_2\text{O}_4$  formation in the initial stage, as described for  $\text{MgO-Al}_2\text{O}_3\text{-fluoride}$  system. The reaction of fluoride with reactants may result in the formation of compounds such as magnesium or iron fluoride. The formation of such compounds results in the lowering of the melting point of LiF (mp  $845^\circ\text{C}$ ) or NaF (mp  $992^\circ\text{C}$ ) by more than  $100^\circ\text{C}$  or  $60^\circ\text{C}$ , respectively (Fig. 4). On the other hand, the melting point of the binary systems such as  $\text{MgO-LiF}$  or  $\text{-NaF}$  and  $\text{Fe}_2\text{O}_3\text{-LiF}$  or  $\text{-NaF}$  nearly agreed with that of pure LiF or NaF. However, X-ray analysis for the products obtained in the DTA experiments did not indicate the formation of compounds such as magnesium or iron fluoride, or Li-, Na-, or Ba-ferrite. This might be due to too small amounts of the compounds for detection by X-ray analysis.

Reijnen<sup>18)</sup> studied the solid state reaction in the  $\text{MgO-Fe}_2\text{O}_3$  system, and proposed two possible mechanisms of counter diffusion of cations for the formation of  $\text{MgFe}_2\text{O}_4$  at a given oxygen pressure and temperature, i.e.  $\text{Mg}^{2+}$  and  $\text{Fe}^{3+}$ , or  $\text{Mg}^{2+}$  and  $\text{Fe}^{3+}$  or  $\text{Fe}^{2+}$  diffuse through the spinel layer. The  $\text{Fe}^{2+}$  diffusion is accompanied by the diffusion of one cation vacancy and by the transport of oxygen in the gas phase. Carter<sup>19)</sup> assumed the mechanism of the counter diffusion of  $\text{Mg}^{2+}$  and  $\text{Fe}^{3+}$ . Lindner<sup>20,21)</sup> reported that the activation energy for the self-diffusion of  $\text{Mg}^{2+}$  in  $\text{MgO}$  single crystal is 79 kcal/mol and that of  $\text{Fe}^{3+}$  in  $\text{ZnFe}_2\text{O}_4$  polycrystal is 82 kcal/mol. These can be regarded as values for the volume or grain boundary diffusion. It was found from the results given in Fig. 3 and Table 1 that the formation rate of  $\text{MgFe}_2\text{O}_4$  in  $\text{MgO-Fe}_2\text{O}_3$  system is controlled by the diffusion with the activation energy of  $70 \pm 4$  kcal/mol, which is comparable to the

above values. Since no  $\text{Fe}^{2+}$  was found in the samples obtained by the isothermal experiments, it seems that  $\text{MgFe}_2\text{O}_4$  formation in  $\text{MgO-Fe}_2\text{O}_3$  system proceeds by the counter diffusion of  $\text{Mg}^{2+}$  and  $\text{Fe}^{3+}$  and that the volume or grain-boundary diffusion is operative in the formation of  $\text{MgFe}_2\text{O}_4$ . The presence of fluorides lowers the value of the activation energy  $E^*$  by 5–13 kcal/mol (Table 1), which might indicate that the fluorides accelerate the diffusion along grain boundary or within bulk. There is a possibility that the dissolution or incorporation of compounds formed by the reaction of fluoride with  $\alpha\text{-Fe}_2\text{O}_3$  into the  $\text{MgFe}_2\text{O}_4$  layer facilitates the diffusion of  $\text{Mg}^{2+}$  or  $\text{Fe}^{3+}$ . It can be considered in the case of LiF or NaF additive that the liquid phase formation at ca.  $700^\circ\text{C}$  or  $800^\circ\text{C}$  accelerates further diffusion by acting as a vehicle of transporting  $\text{MgO}$  or  $\alpha\text{-Fe}_2\text{O}_3$ . It is observed that the lower the  $E^*$  value, the lower the initiation temperature of  $\text{MgFe}_2\text{O}_4$  formation (Fig. 7).

The accelerating mechanism of  $\text{MgFe}_2\text{O}_4$  formation by the presence of chloride was explained as follows:  $\text{MgO}$  particles dissolve in molten chloride to spread uniformly over the outer surface of  $\alpha\text{-Al}_2\text{O}_3$  particles and then  $\text{MgO}$  particles transport into the inner part of  $\alpha\text{-Al}_2\text{O}_3$  particles consisting of crystallites. In the  $\text{MgO-Fe}_2\text{O}_3\text{-NaCl}$  system, discontinuous changes in X-ray diffraction intensities of  $\alpha\text{-Fe}_2\text{O}_3$  and NaCl were observed before melting of NaCl, the initial for mation of  $\text{MgFe}_2\text{O}_4$  beginning simultaneously (Fig. 5-B). The discontinuous changes of X-ray intensities seem responsible for the initial formation of  $\text{MgFe}_2\text{O}_4$ , although no explanation can be given at present. In the case of KCl,  $\text{MgFe}_2\text{O}_4$  was formed after melting of KCl, although a discontinuous change of  $\alpha\text{-Fe}_2\text{O}_3$  intensity was also observed (Fig. 5-C). There may be a difference in the action of solids NaCl and KCl on the  $\text{MgFe}_2\text{O}_4$  formation. It is considered that after chloride melts, the formation of  $\text{MgFe}_2\text{O}_4$  is promoted by the dissolution process of  $\text{MgO}$  particles in molten chloride.

It was found in the high temperature X-ray experiments that  $\alpha\text{-Fe}_2\text{O}_3$  disappears at temperatures where  $\text{MgO}$  still exists (Figs. 5 and 6) and that a trace of  $\text{Fe}^{2+}$  is present in the samples after the experiments. This suggests that a part of  $\text{Fe}^{3+}$  is reduced at high temperatures to ferrous ions by the dissolution of  $\alpha\text{-Fe}_2\text{O}_3$  in  $\text{MgFe}_2\text{O}_4$  phase at relatively high vacuum ( $P_{\text{O}_2}=10^{-1}$  mmHg) in comparison with that in the isothermal experiments ( $P_{\text{O}_2}=10^0\text{--}10^1$  mmHg), and that the  $\text{MgFe}_2\text{O}_4$  formation proceeds by the counter diffusion mechanism of  $\text{Mg}^{2+}$  and  $\text{Fe}^{3+}$  accompanied by partial participation of  $\text{Fe}^{2+}$  in the diffusion, as proposed by Reijnen.<sup>18)</sup>

## References

- 1) B. Delmon, "Reactivity of Solids," ed. by J. S. Anderson, London (1972), p. 567.
- 2) J. Deren, J. Haber, A. Podyorecka, and W. Tur, *Z. Anorg. Allg. Chem.*, **402**, 221 (1973).
- 3) R. Furuichi, T. Ishii, and K. Kobayashi, *J. Thermal Anal.*, **6**, 305 (1974).
- 4) G. Henrich, *Z. Electrochem.*, **58**, 183 (1954).
- 5) H. Schmalzried, *Ber. Dtsch. Keram. Ges.*, **42**, 11 (1969).

- 6) K. J. Mackenzie, *Trans. Brit. Ceram. Soc.*, **63**, 103 (1969).
  - 7) S. Shimada and T. Ishii, *Nippon Kagaku Kaishi*, **1972**, 1234.
  - 8) S. Shimada, R. Furuichi, and T. Ishii, *Bull. Chem. Soc. Jpn.*, **47**, 2026 (1974).
  - 9) S. Shimada, R. Furuichi, and T. Ishii, *Bull. Chem. Soc. Jpn.*, **47**, 2031 (1974).
  - 10) H. Tamura, K. Goto, T. Yotsuyanagi, and M. Nagayama, *Talanta*, **21**, 314 (1974).
  - 11) K. J. Laidler, "Chemical Kinetics," McGraw-Hill, New York (1964), p. 316.
  - 12) W. Jander, *Z. Anorg. Allg. Chem.*, **163**, 1 (1927).
  - 13) B. Serin and R. J. Ellickson, *J. Chem. Phys.*, **9**, 742 (1941).
  - 14) A. M. Ginstling and B. J. Brounshtein, *J. Appl. Chem.*, **23**, 1327 (1950).
  - 15) R. E. Carter, *J. Chem. Phys.*, **34**, 2010 (1961).
  - 16) M. Iwata, *Oyobuturi*, **34**, 812 (1965).
  - 17) S. L. Blum, A. E. Paladino, and L. G. Tubin, *Ceram. Bull.*, **36**, 175 (1957).
  - 18) P. Reijnen, "Reactivity of Solids," ed. by G. M. Schwab, Amsterdam (1965), p. 562.
  - 19) R. E. Carter, *J. Am. Ceram. Soc.*, **44**, 116 (1961).
  - 20) R. Lindner and G. D. Parfitt, *J. Chem. Phys.*, **26**, 182 (1957).
  - 21) R. Lindner, *Z. Electrochem.*, **59**, 967 (1955).
-